This article has been accepted for publication in IEEE Journal of Radio Frequency Identification. This is the author's version which has not been fully edited and content may change prior to final publication. Citation information: DOI 10.1109/JRFID.2026.3687841

Remote Antenna Impedance Estimation Using a UHF RFID Chip

Nicolas Barbot, *Senior Member, IEEE,* Jesse Tuominen, Antti Paukkunen, Jasmin Grosinger, *Senior Member, IEEE,* Pavel Nikitin, *Fellow Member, IEEE,*

***Abstract*—This paper shows that it is possible to estimate the impedance of a remote antenna connected to a UHF RFID chip. The proposed method relies on the measurement of four backscattered field values and the knowledge of only two load impedance values. The field values can be obtained using the autotuning functionality available in modern UHF RFID chips. The method does not make any assumption about the antenna geometry and can be performed multiple times to obtain the impedance of the antenna over a given bandwidth (or any other parameter). More importantly, the method is not limited by the number of autotune capacitors in the chip. The method allows one to directly transform a UHF RFID tag into a sensor if the relation between the antenna impedance and a physical quantity is known. Thanks to the proposed method, a significant part of the UHF RFID tags already deployed in the field can be transformed into sensors.**

***Index Terms*—Green's equation, delta RCS, backscattering communication, RFID, sensing.**

I. Introduction

RFID technology has been deployed in various environments since more than 20 years now and provides a robust way to identify items remotely. The current standard allows one to identify hundreds of tags per second at a distance higher than 10 m.

However, the vast majority of applications for the RFID technology are strictly limited to identification. Sensing is an attractive functionality where a UHF RFID tag can be used to estimate the value of a physical quantity in the vicinity of the tag (*e.g.*, temperature, pressure, presence of gas...) [1]. Over the years, multiples techniques/principles have been used to realize sensing. A popular technique used recently for sensing is to use the autotuning functionality (also called self adjust, self tuning) available in some recent UHF RFID chips [2]. In these chips, a small matching circuit maximizes the power transfer between the antenna and the chip by choosing the best capacitance value among a bank of capacitors. Autotuning is usually done once at each tag power-up and the autotune value is kept constant for the whole inventory round. Moreover, the value of the autotuning capacitance is usually mapped in the tag memory such that it can easily be read using standard access commands (read command).

N. Barbot is with Univ. Grenoble Alpes, Grenoble INP, LCIS, F-26000 Valence, France. P. Nikitin is with Impinj, Seattle, WA, USA. J. Tuominen and A. Paukkunen are with Voyantic, Finland. J. Grosinger is with University of Siegen, Germany.

Using the autotuning functionality (and the associated read command), a lot of authors have tried to realize sensors based on the value of the chosen capacitance. Soon after the publication of the patent [2], academic articles appeared in the literature. Examples, cited in chronological order, includes [3] in which the sensing is done using a RFMicron Magnus S3 chip (with 512 capacitance values) to sense the filling of a canister. This work was later followed by many other papers of the same group [4], [5]. During this period, some other authors have tried to generalize the idea to more common chips such as in [6] (and later extended in [7]), for temperature sensing using a Impinj Monza R6 chip. However, these chips only include five capacitance values which considerably limits the resolution of the sensor. Note that in [8], authors have introduced a dual setup which simplifies the measurement in an unknown environment. Finally, in [9] authors introduced a new technique allowing one to use the autotune value but also to estimate the resonance frequency of the tag to measure the effective permittivity around the tag. Finally, the vast majority of designs are based on the RFMicron Magnus S3 chip due to the high number of capacitance values [3]–[5].

However, all these methods (except [9]) are based on a direct mapping between the physical quantity and the value of the capacitance. The major problem of these techniques is that any external parameter which can affect the capacitance value has to be controlled during the measurement (even if a dual setup such as [8] can be used). This implies that the estimated value is correct only at a given distance, power, in a given environment. Moreover, another drawback is that the RFMicron Magnus S3 chip is not common at all, so the probability to transform an already deployed tag into a sensor is actually quite low in practice.

The technique proposed in this paper allows one to transform any chip with an autotuning circuit into a sensor beyond the limited number of capacitance states. Moreover, the method does not rely on a direct mapping between the capacitance value and the physical quantity but instead, the method estimates the antenna impedance of a remote tag. Then, after the antenna impedance estimation, the physical quantity can be estimated using a classical mapping between the antenna impedance and the physical quantity. Note that the separation between the capacitance value and the physical quantity allows one to design sensors which are only a function of the antenna impedance (independently of the chip used by the sensor or the parameters of the reader). Scripts are also provided as open-source software [10].

Beyond sensing application, the remote antenna impedance

estimation is an interesting research problem on its own. This is especially true for small antennas where the presence of cables (or any other object) can directly modify the antenna characteristics. This is also true for highly reactive (inductive or capacitive) antennas such as UHF RFID antennas because classical instruments with real reference impedance (*e.g.*, 50 Ω) becomes largely inaccurate. Remotely measuring the impedance of an antenna (or the reflection coefficient when connected to a load) in a real environment has been explored by several authors. In [11], the authors determine the antenna impedance using three different loads (open, short and a resistive load) based on Harrington's field decomposition. The same method was adapted in [12] for inductive antennas. Note that these two papers require specific loads values which limits the flexibility of the approach. In [13], the authors succeed to determine the antenna impedance from three different loads (without imposing any specific values). The method has also been applied to sensing application using a 3-load transponder when the sensing affects the antenna impedance, or on a 4-load transponder when the sensing affects load impedance [14]. Finally, note that very innovative and original methods have also been designed for multi-port antennas [15]–[18]. In this paper, we propose a method allowing one to measure the impedance of a (single-port) antenna simply by connecting it to a small UHF RFID chip with autotuning capability to the antenna port. Since the antenna impedance can be estimated remotely, this technique can be used without any cable when the antenna is deployed in its final environment.

The paper is structured as follows: the analytical model and the scientific problem are presented in Section II. A detailed description of the autotuning functionality is presented in Section III. The theoretical contributions of the paper are presented in Section IV, V and VI. Section IV provides the necessary and sufficient condition to be able to estimate the antenna impedance. Then, two different methods allowing one to estimated the antenna impedance in its environment are presented in Sections V and VI. Simulated and measured results, for both methods, are presented in Section VII and VIII respectively. Finally, practical considerations are presented in Section IX before concluding in Section X.

II. Analytical Model

In this section, we expose the model used to characterize the field backscattered by the antenna. This model does not make any assumption on the antenna, and thus remains valid for any antenna.

A. Green's Equation

The backscattered field of loaded antennas has been comprehensively analyzed and understood in the pioneering 1963 doctoral thesis of R. Green [19]. In his thesis, Green successfully decomposes the scattered field of a loaded antenna into a structural mode and an antenna mode:

$$E_s(Z) = E_s(Z_a^*) - \Gamma I(Z_a^*) E_r, \tag{1}$$

where $E_s(Z_a^*)$ is the structural mode component and is independent of the load connected to the antenna, and $-\Gamma I(Z_a^*)E_r$ is the antenna mode component which is a direct function of Γ, with $I(Z_a^*)$ the conjugate current passing through the port, and E_r the field generated by the antenna in transmission. Γ represents the power wave reflection coefficient and is defined as:

$$\Gamma = \frac{Z - Z_a^*}{Z + Z_a}, \tag{2}$$

where Z is the load connected to the antenna port and Z_a is the impedance of the antenna in free space.

The beauty of (1) comes from its graphical representation since all possible backscattered field values correspond to a vector starting from the structural mode $E_s(Z_a^*)$ and ending into a circle of radius $I(Z_a^*)E_r$ (see [19, Fig 7, p.37]).

Even though (1) was originally applied to predict the backscattered field of a loaded antenna in free space, this same equation can still be used in any real environment by considering the antenna and the environment as single (global) antenna. Thus (1) remains valid for an antenna in a real environment (*i.e.*, containing multiple object affecting the propagation). If objects are present in the far-field zone of the antenna, their contributions directly affect the (new) resulting structural mode. If some other objects are present in the near-field region of the antenna, they impact the backscattered field in the (new) structural mode, but also in the (new) antenna mode:

$$E'_s(Z) = E'_s(Z'^*_a) - \Gamma' I'(Z'^*_a) E'_r. \tag{3}$$

Unlike (1), note that the $'$ is used in (3) to denote the different quantities when the antenna is placed in a real (non-free-space) environment. Finally and more importantly, this model is valid for any real environment.

B. Problem Statement

Now that the model is established, the problem that we are trying to solve can be summarized as: assuming we can measure the scattered field $E'_s(Z_i)$ for different load values Z_i, can we find a procedure allowing one to estimate the antenna impedance Z'_a (in its environment). Moreover, could we implement the technique using off-the-shelf UHF RFID chips (with or without autotuning capabilities). The estimation of Z'_a ultimately allows anyone to transform a classical tag into a sensor if the variation between Z'_a and the physical quantity is known. Note that in (3), $E'_s(Z'^*_a)$ and $I'(Z'^*_a)E'_r$ are unknown (in addition to Z'_a).

In regard of this scientific problem, the first contribution of this article is to determine the necessary and sufficient conditions allowing one to estimate Z'_a (see Section IV). Two different methods allowing one to estimated the antenna impedance in its environment are presented. The first method is not a contribution of this article and has been derived in [20] and is based on the measurement of three field values and the knowledge of three loads. This method is presented in this paper for completeness under the name "3-Reference Method" (see Section V) but remains mainly incompatible with the UHF RFID technology. The second method, which is the main contribution of this article, is based on the measurement of four field values, and the knowledge of only two different loads. This method is presented under the name "4-Reference

Method" (see Section VI). This method is compatible with the UHF RFID technology and allows one to estimate the antenna impedance form any (recent) tag.

III. Autotuning

The autotuning functionality (also called self adjust, self tuning) allows recent chips to change their input impedance to maximize the power transfer efficiency. From an hardware point of view, the circuit is mainly composed of a bank of capacitor and some logic to monitor the voltage at the output of the rectifier. When an RFID reader is generating a continuous wave, the autotuning circuit is activated (before the activation of the chip) and tries to maximize the power transfer between the antenna and the chip by choosing the best capacitance value among the bank of capacitors. The autotuning is usually done once at each tag power-up and the autotune value is kept constant for the whole inventory round. Moreover, the value of the autotuning circuit is usually mapped in the tag memory such that the value can be easily accessed using standard access commands (*e.g.*, read command).

Note that at a given power level and a given frequency, an off-the-shelf tag with an autotuning functionality can switch its impedance between $2N$ different states, with N the number of capacitance values in the chip. These states are the N states in the absorbing state, plus N states in the reflecting state (when the tag is modulating). However, not all these states can be achieved during an inventory round because the chosen capacitance can not be controlled easily. In a given configuration, only 4 different states can be achieved. The first state corresponds to the impedance of the tag in the default state Z_1 which can be modeled by a resistance in parallel with a capacitor [21] (for an improved accuracy, an additional capacitance due to adhesive and antenna mount parasitics can also be added here). More importantly, note that this default impedance value is given in the chip datasheet. The second state corresponds to the reflecting state and can be modeled as the default impedance Z_1 in parallel with a modulation resistance. In this paper, we consider that this modulation resistance is a complex impedance noted Z_R. The third and forth states corresponds to the default and reflecting state of the chip but when the autotuning functionality is activated. Note that these two last states are different compared to the two former ones since the capacitor of the autotuning is placed in parallel with the impedance of the chip without autotune. The capacitance value of the autotuning circuit can be positive (*i.e.*, total capacitance in increased) or negative (*i.e.*, total capacitance in decreased). The four different states of a UHF RFID chip with an activable autotune are presented in Fig. 1.

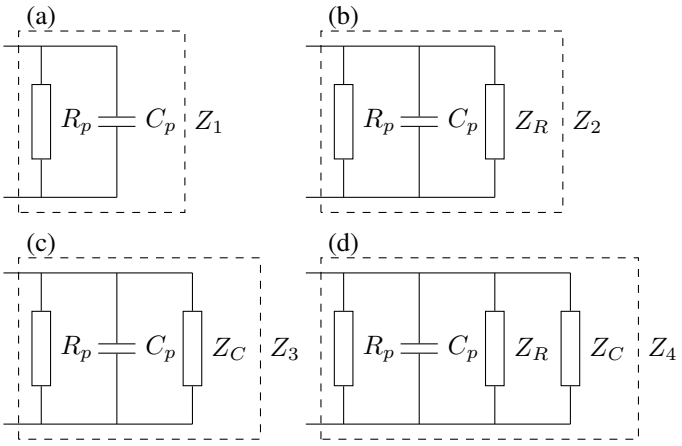

Fig. 1. The four different states of a UHF RFID tag with autotuning. (a) Default state, (b) reflecting state, (c) default state with autotune and (d) reflecting state with autotune.

IV. Requirements for Z'_a Estimation

From (3), we can see since $E'_s(Z'^*_a)$, $I'(Z'^*_a)E'_r$ and Z'_a are unknown, that we need at least three observations of the backscattered field values for three known load values. Consequently, if a UHF tag has only 2 states (*i.e.*, 2 impedance values) then there is no method allowing one to recover the antenna impedance value from the observation and knowledge of only two states. Thus, it is impossible to determine the antenna impedance with any method based on only two references. This result applies to every tag which do not have the autotuning functionality.

V. 3-Reference Method

Assuming that a given tag has an autotuning capability, the following method allows one to estimate the antenna impedance in its environment using three known loads and three measured backscattered fields. This method has been described in [20] but is shortly recalled here for clarity and completeness. Note that these three loads can be any 3-combination of the four loads presented in Fig. 1.

The estimation of Z'_a requires the knowledge of three loads and the three associated observed field values. Assuming the three impedance values Z_1, Z_2 and Z_3 known, and associated observed field values E_{s1}, E_{s2} and E_{s3} and by noticing that (3) remains valid for each couple (Z_i, E_{si}). Then, by doing the difference between two (different) measurements, we have:

$$E'_{s1} - E'_{s3} = -(\Gamma'_1 - \Gamma'_3)I'(Z'^*_a)E'_r \tag{4}$$

$$E'_{s2} - E'_{s3} = -(\Gamma'_2 - \Gamma'_3)I'(Z'^*_a)E'_r \tag{5}$$

where one can note that the structural mode $E(Z^*_a)$ has been suppressed. Moreover, by doing the ratio between (4) and (5):

$$\frac{E'_{s1} - E'_{s3}}{E'_{s2} - E'_{s3}} = \frac{\Gamma'_1 - \Gamma'_3}{\Gamma'_2 - \Gamma'_3}, \tag{6}$$

where one can also note that the multiplicative term $-I'(Z'^*_a)E'_r$ has been suppressed. By developing Γ' in (6) using (2) (with respect to Z'_a):

$$\frac{E'_{s1} - E'_{s3}}{E'_{s2} - E'_{s3}} = \frac{Z_2 + Z'_a}{Z_1 + Z'_a} \cdot \frac{Z_1 - Z_3}{Z_2 - Z_3}. \tag{7}$$

Finally, by isolating Z'_a, we have:

$$Z'_a = \frac{(E_{s2} - E_{s3})(Z_1 - Z_3)Z_2 - (E_{s1} - E_{s3})(Z_2 - Z_3)Z_1}{(E_{s1} - E_{s3})(Z_2 - Z_3) - (E_{s2} - E_{s3})(Z_1 - Z_3)} \tag{8}$$

First, note that the method is defined only if the capacitance value of the autotune is different than 0 fF (if $Z_C = \infty$ then $Z_1 = Z_3$ and $Z'_a = -Z_1$ which represents a non-physical antenna). Second, the method provides the same estimation even if each field value multiplied by a complex constant *i.e.*, rotation and scaling, and/or if each field value is added with a complex constant *i.e.*, translation. Thus the 3-reference presents a rotational invariance and translational invariance. This constitutes a significant advantage under strong structural mode scattering (translation) and/or propagation impairments (rotation). Finally, even if this method is elegant, the implementation of the method using a UHF RFID chip is hard in practice since we need to know three impedance values. Even with a tag with autotuning, only Z_1 and Z_3 are known. Note that Z_2 and Z_4 are not accurately known since the value of Z_R is not accurately known (Z_R is not indicated in public datasheets). Thus to apply the 3-reference method, one has to arbitrary choose the Z_R value. In practice, a value between 10 and 50 Ω can be chosen with an imaginary part equals to zero [22]. Thus, this method remains mainly incompatible with the use of UHF RFID tags.

VI. 4-Reference Method

In order to solve the limitation of the 3-reference method *i.e.*, the assumption of an arbitrary Z_R value, the 4-reference method is now presented. This method allows one to estimate Z'_a from the measurement of four loads values of which only two are known, without any other assumption. As seen in Fig. 1, a tag with autotuning capability can switch its impedance between four values:

$$\begin{cases} Z_1 = R_p // C_p \\ Z_2 = Z_1 // Z_R \\ Z_3 = Z_1 // Z_C \\ Z_4 = Z_1 // Z_R // Z_C \end{cases} \tag{9}$$

Note that Z_1 is known from the datasheet, Z_3 is known from the datasheet and by reading the tag memory (when autotune is enabled). Z_2 and Z_4 are usually not known because the value of Z_R is not indicated in the datasheet.

To simplify the equations, it is easier to think in term of admittance:

$$\begin{cases} Y_1 = 1/Z_1 \\ Y_2 = Y_1 + Y_R \\ Y_3 = Y_1 + Y_C \\ Y_4 = Y_1 + Y_R + Y_C \end{cases} \tag{10}$$

Note that Y_1 and Y_3 are known, Y_2 and Y_4 are supposed to be unknown. By subtracting E'_{s1} and E'_{s2}:

$$E'_{s1} - E'_{s2} = -(\Gamma'_1 - \Gamma'_2) I'(Z'^*_a) E'_r. \tag{11}$$

Doing the same with E'_{s3} and E'_{s4}:

$$E'_{s3} - E'_{s4} = -(\Gamma'_3 - \Gamma'_4) I'(Z'^*_a) E'_r. \tag{12}$$

Dividing the two previous quantities leads to:

$$\frac{E'_{s1} - E'_{s2}}{E'_{s3} - E'_{s4}} = \frac{\Gamma'_1 - \Gamma'_2}{\Gamma'_3 - \Gamma'_4}. \tag{13}$$

Note that Γ' can also be expressed as a function of Y and Y'_a. By replacing Z by $1/Y$ and Z'_a by $1/Y'_a$, we can write:

$$\Gamma' = \frac{Z - Z'^*_a}{Z + Z'_a} \tag{14}$$

$$= \frac{Y'^*_a - Y}{Y'_a + Y} \cdot \frac{Y'_a}{Y'^*_a}. \tag{15}$$

Developing Γ' as a function of Y:

$$\frac{E'_{s1} - E'_{s2}}{E'_{s3} - E'_{s4}} = \frac{Y_2 - Y_1}{Y_4 - Y_3} \cdot \frac{(Y_3 + Y'_a)(Y_4 + Y'_a)}{(Y_1 + Y'_a)(Y_2 + Y'_a)} \tag{16}$$

$$= \frac{(Y_3 + Y'_a)(Y_4 + Y'_a)}{(Y_1 + Y'_a)(Y_2 + Y'_a)} \tag{17}$$

$$= A. \tag{18}$$

Repeating the same development from (11) to (18) but inverting E'_{s2} and E'_{s3} leads to:

$$\frac{E'_{s1} - E'_{s3}}{E'_{s2} - E'_{s4}} = \frac{Y_3 - Y_1}{Y_2 - Y_4} \cdot \frac{(Y_2 + Y'_a)(Y_4 + Y'_a)}{(Y_1 + Y'_a)(Y_3 + Y'_a)} \tag{19}$$

$$= \frac{(Y_2 + Y'_a)(Y_4 + Y'_a)}{(Y_1 + Y'_a)(Y_3 + Y'_a)} \tag{20}$$

$$= B. \tag{21}$$

where the second line of both equation holds because Y_C and Y_R are in parallel. The product between A and B is equal to:

$$A \cdot B = \frac{(Y_4 + Y'_a)^2}{(Y_1 + Y'_a)^2}. \tag{22}$$

The ratio between A and B is equal to:

$$A/B = \frac{(Y_3 + Y'_a)^2}{(Y_2 + Y'_a)^2}. \tag{23}$$

Taking the square root of the 2 previous quantities:

$$\sqrt{A \times B} = \frac{Y_4 + Y'_a}{Y_1 + Y'_a}, \tag{24}$$

$$\sqrt{A/B} = \frac{Y_3 + Y'_a}{Y_2 + Y'_a}. \tag{25}$$

Developing the Y values:

$$\sqrt{A \times B} = \frac{Y_1 + Y_R + Y_C + Y'_a}{Y_1 + Y'_a}, \tag{26}$$

$$\sqrt{A/B} = \frac{Y_1 + Y_C + Y'_a}{Y_1 + Y_R + Y'_a}. \tag{27}$$

From (26) and (27), isolating Y_R in (26):

$$Y_R = (\sqrt{A \times B} - 1)(Y'_a + Y_1) - Y_C. \tag{28}$$

Re-injecting Y_R into (27) and isolating Y'_a

$$Y'_a = \frac{Y_1(1 - \sqrt{A/B}\sqrt{A \times B}) + Y_C(1 + \sqrt{A/B})}{\sqrt{A/B}\sqrt{A \times B} - 1}. \tag{29}$$

Be careful here that, in the complex domain $\sqrt{A \times B}$ is not always equal to $\sqrt{A} \times \sqrt{B}$. Finally, Z'_a can be obtained with:

$$Z'_a = \frac{1}{Y'_a}. \tag{30}$$

Thus, the method allows one to estimate the antenna impedance from the knowledge of only two different loads

This article has been accepted for publication in IEEE Journal of Radio Frequency Identification. This is the author's version which has not been fully edited and content may change prior to final publication. Citation information: DOI 10.1109/JRFID.2026.3687841

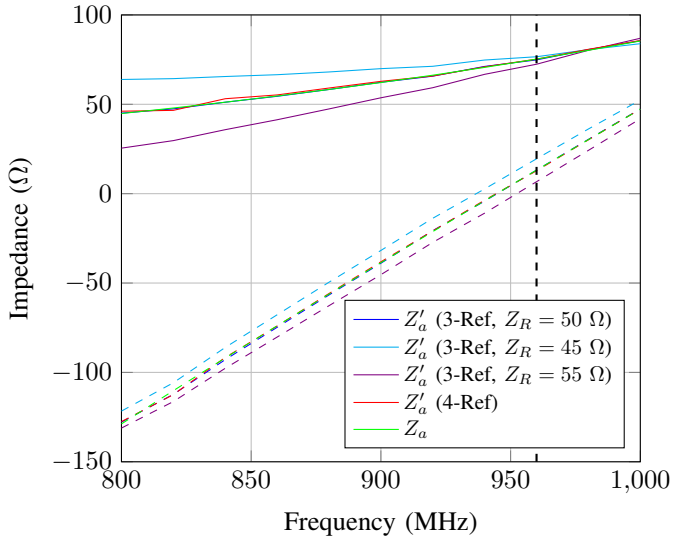

Fig. 2. Simulated results for the 3-references method and for the 4-reference method for a classical dipole antenna. Real part in plain line, imaginary part in dashed line.

and the measurement of four backscattered field values. Note that the method is defined only if the capacitance value of the autotune circuit is different than 0 (if $Y_C = 0$ then $Z'_a = -Z_1$ which represents a non-physical antenna).

Moreover this technique provides the same estimation even if each field value multiplied by a complex constant *i.e.* rotation and scaling, and/or if each field value is added with a complex constant *i.e.* translation. Thus the 4-reference presents a rotational invariance and translational invariance. This constitutes a significant advantage under strong structural mode scattering (translation) and/or propagation impairments (rotation).

Independently, note that if one isolate Y'_a in (26) (instead of isolating Y_R) and then re-inject it into into (27), then the method allows one to estimate Y_R (in real and imaginary parts) remotely.

VII. Simulation

A. Antenna Impedance Estimation

In order to validate the accuracy of the proposed expressions, an electromagnetic simulation has been realized using the NEC-2 software. NEC-2 is a open source full-wave electromagnetic solver based on Method of Moments. The considered wire antenna is a classical half-wavelength dipole antenna of length 15 cm impinged by a plane wave with vertical polarization. This antenna is then loaded with lumped element of known impedance. These impedance values have been extracted directly from the Impinj Monza R6 datasheet, assuming an autotuning capacitance of $Z_C = +100$ fF (maximum value) and the modulation resistance have been set to $Z_R = 50$ Ω (without imaginary part).

Estimation of Z'_a is done using the 3-reference method using Z_1, Z_2, and Z_3 (see Fig.1) and the 4-reference method using Z_1, Z_2, Z_3, and Z_4 (see Fig.1). The estimated values can be compared to the impedance of the antenna Z_a. This impedance is obtained by an independent simulation with a voltage source connected to the port of the antenna. Note that since both simulations are done in free space, $Z_a = Z'_a$ (see Section II.A).

Results are presented in Fig. 2. The antenna impedance Z_a can be easily recognized since at the resonance the dipole antenna at is obtained at $0.48\,c/l = 960$ MHz. At this frequency the impedance of the antenna is close to 73 Ω. This impedance is indicated with a vertical black dashed line at 960 MHz. The imaginary part is slightly higher than the theoretical value due to the finite diameter of the dipole (1 mm). For all frequencies, both methods, *i.e.*, 3-reference method and 4-reference method are able to perfectly estimate the antenna impedance (in both real part and imaginary part) even if the impedance of this dipole presents a significant mismatched compared to the impedance of the Impinj Monza R6 chip (at 960 MHz, this mismatch corresponds to $|\Gamma_1| = 0.91$). Finally, for the 3-reference method, when the modulation resistance is not perfectly known (see curve with $Z_R = 45$ Ω and $Z_R = 55$ Ω, the antenna impedance estimation becomes erroneous (in both real part and imaginary part).

B. Sensitivity Analysis

A sensitivity analysis has been conducted for both methods (3-reference method and 4-reference method) using a Monte Carlo simulation. The general principle of this simulation is as follows: first we determine the four known impedance values from the Monza R6 datasheet (and by setting $Z_R = 50$ Ω and choosing $Z_C = -100$ fF). Then, for a given Z_a value, we predict the four field values according to (3) (assuming fixed $E'_s(Z'^*_a) = 1$ and $I'(Z'^*_a)E'_r = 1$)). A small amount of complex additive white gaussian noise is then added on the four field values (corresponding to a SNR = 43 dB). Finally, we estimate the antenna impedance (using the 3-reference method and the 4-reference method) for a large number of independent realizations of the complex noise and we compare the results with the true value of Z_a. This process is repeated all Z_a values. Note that no electromagnetic simulation is involved in the process. Results are presented in Fig. 3 in term of accuracy of the estimator (defined as $|E(Z'_a) - Z_a|$) and the precision of the estimator (defined as var(Z'_a) in dB).

Note that both methods present a good accuracy (see blue zone on the two top plots). The accuracy is degraded when the antenna impedance has a strong negative imaginary part (capacitive antenna). For the precision, both method have a better precision when the antenna impedance has a small real part and a high positive imaginary part (inductive antenna). Surprisingly, both methods present a very similar performance in term of accuracy and precision (despite of the difference in the analytical derivations).

VIII. Measurement

A. Tags Under Test

Three different tags are considered in this study. The first tag is a E62 tag on a wet inlay. This tag is based on a dipole antenna, the matching is ensured using a T-match and the chip is a Impinj Monza R6 chip. The second tag is also based on a Monza R6 chip but the antenna is a slot based antenna on

This article has been accepted for publication in IEEE Journal of Radio Frequency Identification. This is the author's version which has not been fully edited and content may change prior to final publication. Citation information: DOI 10.1109/JRFID.2026.3687841

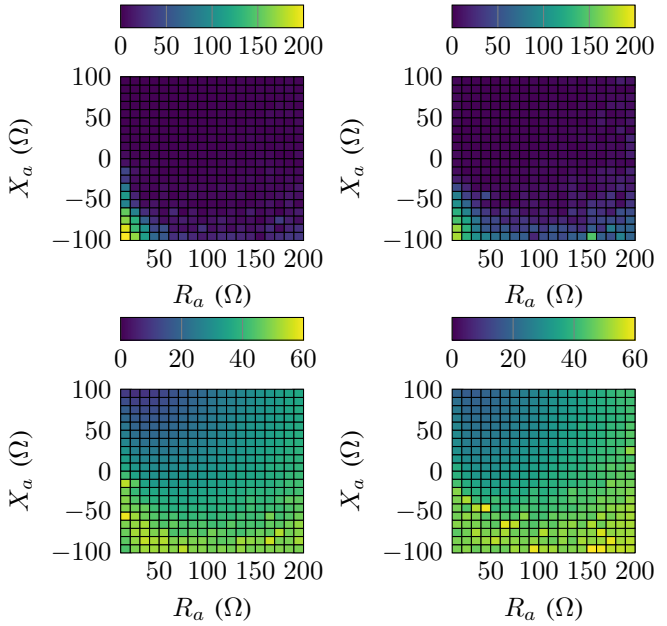

Fig. 3. Performance of the 3-reference method (left column) and 4-reference method (right column). For both methods, accuracy defined as $|E(Z'_a) - Z_a|$ (top line), and precision defined as $\text{var}(Z'_a)$ in dB (bottom line) as a function of the true antenna impedance value Z_a. All results are obtained at 915 MHz.

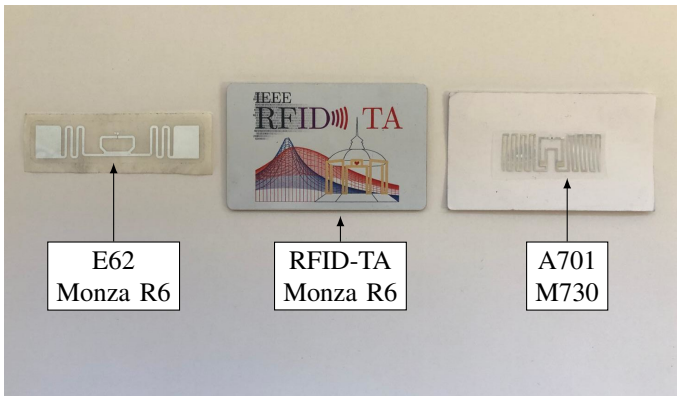

Fig. 4. Tags under test to estimate the impedance of the antenna using the proposed method.

FR4 substrate. This tag was designed for the IEEE RFID-TA 2025 conference. Finally, the third tag is a A701 on a dry inlay with a Impinj M730 chip. The antenna is based on a dipole antenna with a T-match structure. The tag is taped on a paper sheet. A picture of the three tags is presented in Fig. 4.

B. Measurement Bench

The measurement bench used in this paper is based on a Voyantic Tagformance reader placed in an anechoic chamber. The Tagformance reader with standard frequency range option is able to characterize a tag in a bandwidth between 800 MHz and 1 GHz. Other prototype such as [23] can also be used (as long a the In-phae (I) and Quadrature (Q) channels are available to the user).

The procedure allowing one to estimate the impedance of the antenna remotely is described in Algorithm 1. The reading

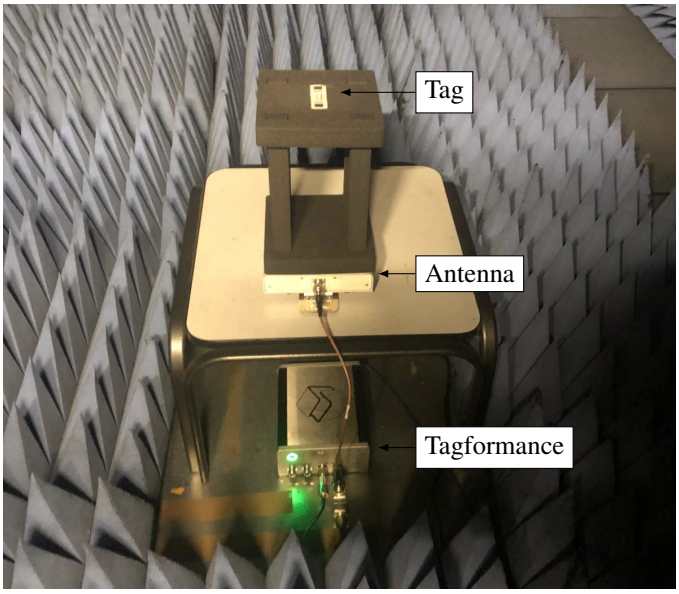

Fig. 5. Measurement bench used to remotely estimate the antenna impedance of a tag using the 3-reference method and the 4-reference method.

Algorithm 1 Remote antenna impedance estimation using the 4-reference method.

Require: Z_1
  Read the capacitance value
  if $Y_C \neq 0$ **then**
    Disable autotuning
    Measure E'_{s1} and E'_{s2}
    Enable autotuning
    Measure E'_{s3} and E'_{s4}
    Compute A, B with (18) and (21)
    Compute Z'_a with (29) and (30)
  end if

of the capacitance value requires the issue of a read command at a specific address (this address is chip specific) and the mapping between the value and the capacitance is also chip specific. This command can be sent at the minimum power needed to activate the chip. The measurement of E'_{s1} and E'_{s2} is realized by sending a Query command at the minimum power needed to activate the chip, on successful reception, the tag will backscatter its RN16 and E'_{s1} and E'_{s2} can be sampled inside the tag preamble (without any averaging). The measurement of E'_{s3} and E'_{s4} follows the exact same procedure. Note that this procedure can be repeated multiple time to obtained the antenna impedance as a function of any parameter (frequency, time...). In the following, the antenna impedance is computed over the frequency band of 800 MHz to 1 GHz in anechoic chamber.

C. Antenna Impedance Estimation

The first step of the procedure (see Algorithm 1) requires to read the capacitance value of the autotuning circuit. Note that the associated bits are located at the address `0x0E` for the Monza R6 chip and at the address `0x14` for the M700 series

This article has been accepted for publication in IEEE Journal of Radio Frequency Identification. This is the author's version which has not been fully edited and content may change prior to final publication. Citation information: DOI 10.1109/JRFID.2026.3687841

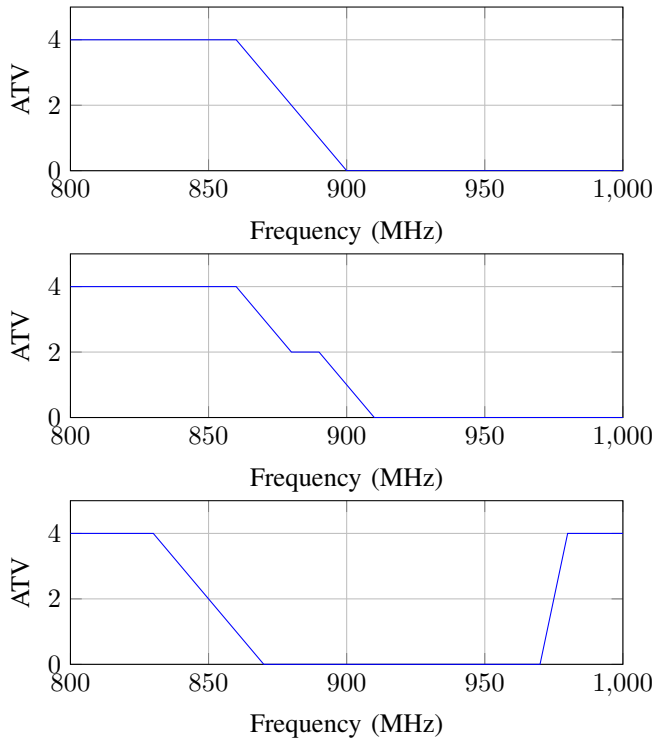

Fig. 6. Reading of the AutoTuning Value (ATV) as a function of the frequency for the three considered tags: (a) E62 tag, (b) IEEE RFID-TA 2025 tag, (c) A701 tag.

TABLE I
MAPPING BETWEEN ATV BITS AND CHANGE IN CAPACITANCE VALUE (FF).

ATV	Monza R6	Monza R6 A/B/P	M700	M800
0	−100	−80	−100	−100
1	−60	−40	−40	−40
2	0	0	0	0
3	60	60	40	40
4	100	100	100	100

and M800 series chips and can be accessed using a classical read command. Fig. 6 presents the value of the ATV bits for the three different tags over the whole frequency band (with a step of 10 MHz).

The mapping between the ATV value and the capacitance value is provided in the public datasheet of each chip. Table I summarizes the results for all chips.

From the observation of Fig. 6 and Table I, one can now estimate the capacitance value. Note that the antenna impedance estimation (for both 3-reference method and 4-reference method) requires that $Y_C \neq 0$. From Fig. 6, we can see that this condition appears at 880 MHz for the E62 tag, at 880 and 890 MHz for the RFID-TA 2025 tag and at 850 MHz for the A701 tag. For all the other frequency points, both methods can be applied and antenna impedance estimation can be computed.

The second step of the procedure requires the measurement of the four field values (E'_{s1} and E'_{s2} without autotune and, E'_{s3} and E'_{s4} with autotune). The (sampled) field backscattered

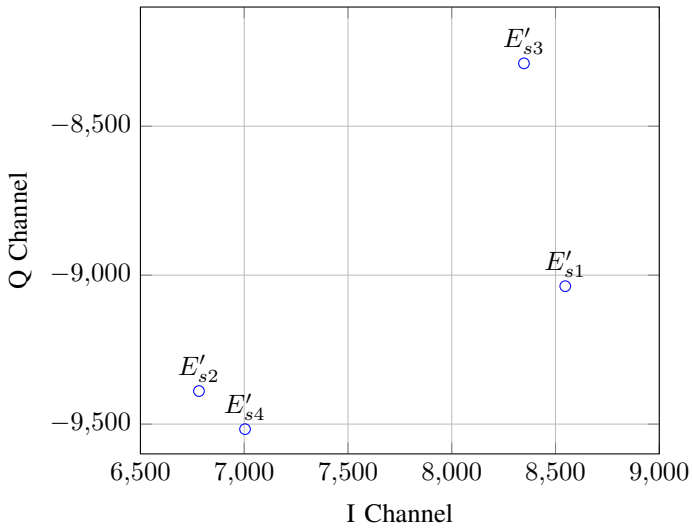

Fig. 7. IQ plane of the backscattered field by the E62 tag at 900 MHz without autotuning (E'_{s1} and E'_{s2}) and with autotuning (E'_{s3} and E'_{s4}).

by a tag is presented in Fig. 7 for the E62 at 900 MHz. The variation between E'_{s1} and E'_{s2} (response without autotuning) can easily be detected by the reader. Same observation holds between E'_{s3} and E'_{s4} (response with autotuning). Note that the variation between between E'_{s2} and E'_{s4} can be quite small in practice which require significant care during the measurement.

Moreover, note that the Tagformance does not provide the I and Q channels in V/m (neither in V) but directly in the number of steps of the analog to digital converters. Note that the unit chosen by the reader does not impact the estimation of the antenna impedance since both methods are based on the ratio of a difference between the signals [see (6) for the 3-reference method and (18) and (21) for the 4-reference method].

Finally, using both the measured field values and the autotune capacitance value, one can estimate the impedance of the tag antenna remotely. Results are presented respectively in Fig. 8, 9 and 10 for the E62, the IEEE RFID-TA 2025 tag and the A701 tag for the 3-reference method (assuming $Z_R = 50\ \Omega$) and the 4-reference method. Moreover, note that both methods are applied on the exact same data points (same field values, same ATV values).

For the E62 tag, the estimated antenna impedance versus frequency is presented in Fig. 8 for the 3-reference and the 4-reference method. Simulation of the tag antenna has also be realized using CST Microwave Studio (see [22] for a detailed description of the antenna) in free space. The estimation of the real part of the antenna impedance is in a very good agreement with the simulation. The imaginary part experiences more differences (especially at higher frequencies). Note that, the antenna impedance estimation is not defined at 880 MHz since the ATV value corresponds to 0 fF [see Fig.6(a) and Table I].

The same results are presented for the IEEE RFID-TA 2025 tag. The simulation has been realized using the frequency solver of CST Microwave Studio. Here, both methods are able

This article has been accepted for publication in IEEE Journal of Radio Frequency Identification. This is the author's version which has not been fully edited and content may change prior to final publication. Citation information: DOI 10.1109/JRFID.2026.3687841

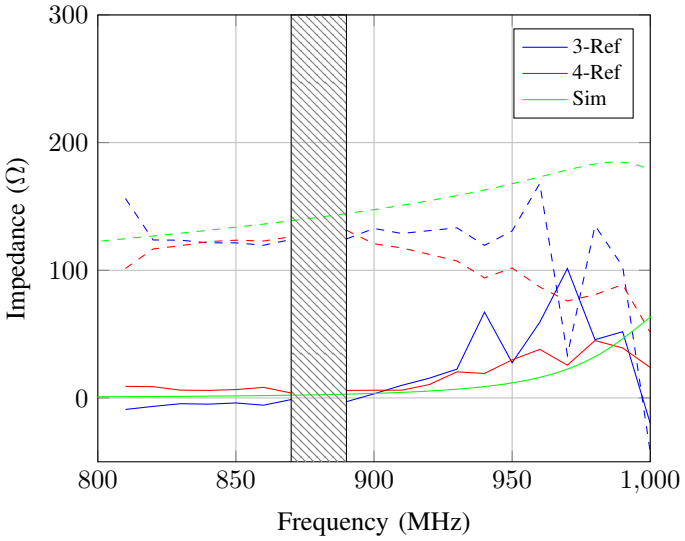

Fig. 8. Estimated antenna impedance for the E62 tag in measurement and simulation. Real part in plain line, imaginary part in dashed line. The 3-reference and 4-reference methods are not defined at 880 MHz since the autotune value corresponds to 0 fF.

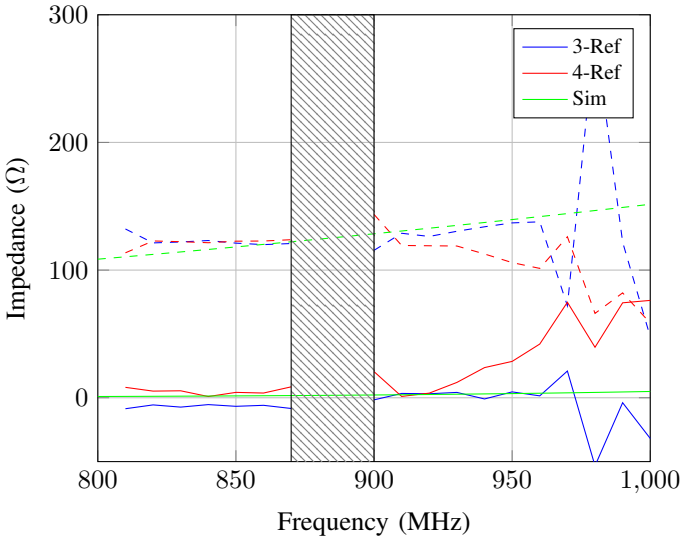

Fig. 9. Estimated antenna impedance for the IEEE RFID-TA 2025 tag in measurement. Real part in plain line, imaginary part in dashed line. The 3-reference and 4-reference methods are not defined at 880 MHz and 890 MHz since the autotune value corresponds to 0 fF.

to correctly estimate the antenna impedance in the lower part of the frequency band. The accuracy of the 4-reference method seems to decrease at higher frequencies. Note that, the antenna impedance estimation is not defined at 880 and 890 MHz since the ATV value corresponds to 0 fF ([see Fig.6(b) and Table I].

Finally, for the A701, note that the simulation predicts a significant variation in both real part and imaginary part. In addition, the antenna impedance of a similar tag, E702, has been measured using the imaging theory technique in [24, p. 143, Fig. 2] for a comparison between simulation and measurement. The 3-reference method is able to provide a correct estimation of the antenna impedance in both real part

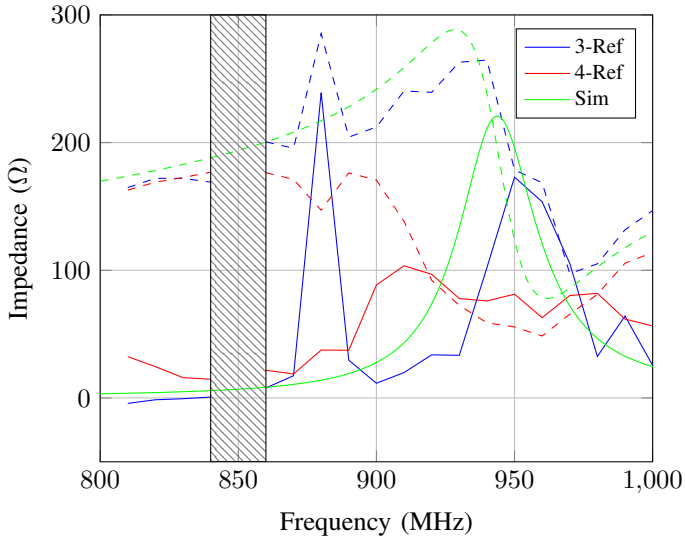

Fig. 10. Estimated antenna impedance for the A701 tag in measurement. Real part in plain line, imaginary part in dashed line. The 3-reference and 4-reference methods are not defined at 850 MHz since the autotune value corresponds to 0 fF.

and imaginary part over the whole frequency band (except for 870 MHz). The 4-reference method provides a lower quality estimation (but is not impacted at 870 MHz). Note that, the antenna impedance estimation is not defined at 850 MHz since the ATV value corresponds to 0 fF [see Fig.6(c) and Table I].

D. Sensing

For a proof of concept, we apply here the 3-reference method and the 4-reference method to estimate the change of the antenna impedance when a UHF RFID tag is touching an external object. Note that this object is a rectangular piece of polycarbonate of dimension $5 \times 5 \times 2$ cm (theoretical permittivity around 3) placed directly on top of the tag. The whole setup is placed in the anechoic chamber. This object can represent the hand of the user in a human-computer interaction. The objective is to detect the presence or absence of the object on the tag. The tag considered in this study is the E62 tag. Note that the antenna of this tag has not been optimized for sensing application.

Five successive measurements of the tag are realized without the object and five measurements are realized with the object on top of the tag. Moreover the ATV values are read in each case. Note that, the 3-reference method (assuming $Z_R = 50\,\Omega$) and the 4-reference method are applied on the exact same measured fields and capacitor values (and no averaging techniques has been used). Note that during an estimation *i.e.*, measurement of the four field values (and the ATV value), the sensing parameter (and the parameters associated to the setup) need to be kept constant. They can however be changed (in theory) between successive estimations.

Results are presented in Fig. 11 where we can see the estimated impedance Z'_a in the complex plane. Note that both estimations when the object is not present are relatively close. When the object is placed on the tag, the estimation of the tag

This article has been accepted for publication in IEEE Journal of Radio Frequency Identification. This is the author's version which has not been fully edited and content may change prior to final publication. Citation information: DOI 10.1109/JRFID.2026.3687841

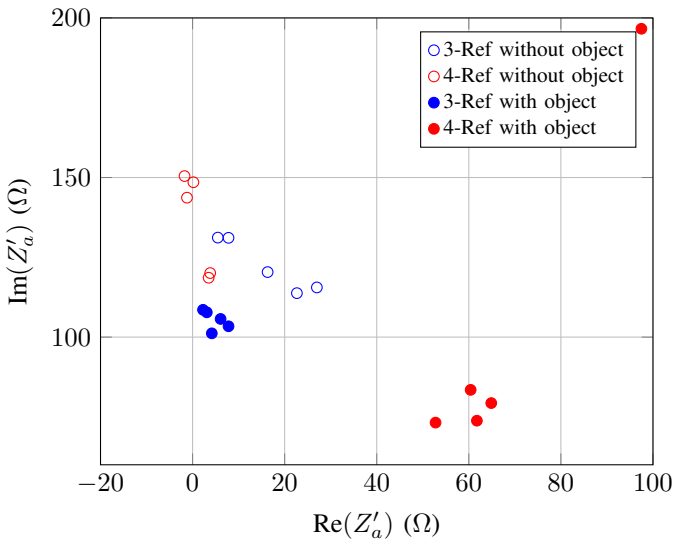

Fig. 11. Impedance of the antenna as a function of the presence of a plastic object on top of the tag for the 3-reference method and 4-reference method. Five measurements without the object and five measurements with the object.

TABLE II
MEAN VALUE AND VARIANCE OF THE ESTIMATORS.

	Mean 3-Ref	Mean 4-Ref
Without object	$15.8 + 122i$	$0.903 + 136i$
With object	$4.68 + 105i$	$67.5 + 101i$

	Var. 3-Ref	Var. 4-Ref
Without object	155.27	252.02
With object	14.443	3158

impedance is different for the two methods which can indicate that the methods can be sensitive to noise. Moreover, one of the estimation for the 4-reference method provide an estimation very different compared to the four other estimations.

The same results are also presented in term of mean value and variance in Table II. where we can confirm that the methods remain sensitive to noise.

Despite these drawbacks, note that the presence of the object can be detected by both methods. Finally, the accuracy of the proposed methods can be increased by using averaging techniques and/or specific antenna design. Another approach can be based on signal-pattern based sensing [25] which can offer an additional robustness to the approach.

IX. CONSTRAINTS AND PERSPECTIVES

As stated in Section VI, the 4-reference method relies on the knowledge of two impedance values and the measurement of four field values. For the moment, the method can be used with Impinj Monza R6, Impinj Monza R6 A/B/P, Impinj M700 series, and Impinj M800 series chips. There are other recent chips which also include an autotuning circuitry however they are not strictly compatible with the proposed method. For example, RFMicron Magnus S2, and RFMicron Magnus S3 chips have an autotuning circuit composed of 512 capacitors values, the selected capacitor can be read in the tag memory however the autotuning, from the authors' knowledge, can not be deactivated. The NXP UCODE8 and NXP UCODE9 chips have small autotuning circuits composed of 3 capacitors, moreover, the autotuning functionality can be enabled and disabled, however, from the authors' knowledge, the capacitance value is not mapped in the tag memory. In these 2 examples, the proposed method needs to be slightly adjusted if someone want the estimate the antenna impedance remotely.

About the non-linearity behavior of the chip, note that the proposed procedures (3-reference method and 4-reference method) can, in theory, be realized at any incident power (if the tag is purely linear). However in practice, tags are non-linear devices and the impedance in the default state as indicated in the datasheet is valid only at the activation power. Consequently, all backscattered field values have to be measured at this same activation power and the antenna impedance estimation is valid (only) at this specific power.

In a multiple tags scenario, the proposed methods (3-reference method and 4-reference method) can, in theory, estimate the antenna impedance of any specific tag in the total population if the field values are measured in the preamble of the EPC reply (instead of the RN16) of the given tag. This property allows ones to transform an already deployed tag population into a real wireless sensor network.

On the reader side, note that any reader which has access to the I and Q channels of the receiving path can be used to implement the 3-reference method and the 4-reference method. So in theory, any reader based on an IQ demodulator can be used to estimate the impedance of the tag antenna using the proposed method. However, the I and Q channels need to be available to the user and very few industrial readers gives access to this information. Software defined readers can easily be used to implement the proposed techniques [26].

X. CONCLUSION

This paper provides a method to remotely estimate the impedance of an antenna. The method requires two known loads and four measured backscattered field values. These requirements can be provided by (almost) any UHF RFID chip with an autotuning capability. The technique could allow one to transform a classical tag into a sensor if the relation between the antenna impedance and the physical quantity is known.

XI. ACKNOWLEDGMENT

This work was supported by a grant from the French government, managed by the French National Research Agency (ANR) under the France 2030 program, grant number "ANR-24-RRII-0002", and implemented by the Inria Quadrant Programme.

REFERENCES

[1] J. Grosinger and A. Michalowska-Forsyth, "Space tags: Ultra-low-power operation and radiation hardness for passive wireless sensor tags," *IEEE Microwave Magazine*, vol. 23, no. 3, pp. 55–71, Mar. 2022.

[2] S. Rokhsaz, B. D. Young, and A. Younis, "Method and apparatus for sensing environmental parameters using wireless sensor (s)," U.S. Patent 9,991,596, Jun. 5, 2018, filed in 2015.

[3] M. C. Caccami and G. Marrocco, "Electromagnetic characterisation of self-tuning UHF RFID tags for sensing application," in *2016 IEEE International Symposium on Antennas and Propagation (APSURSI)*, Fajardo, PR, Jun. 2016, pp. 1273–1274.

[4] F. Naccarata, G. M. Bianco, and G. Marrocco, "Sensing performance of multi-channel RFID-based finger augmentation devices for tactile internet," *IEEE Journal of Radio Frequency Identification*, vol. 6, pp. 209–217, May 2022.

[5] F. Nanni, S. Nappi, and G. Marrocco, "Potentiometric sensing by means of self-tuning RFID ICs," in *2022 IEEE International Conference on RFID (RFID)*, Las Vegas, NV, May 2022, pp. 17–22.

[6] K. Zannas, H. E. Matbouly, Y. Duroc, and S. Tedjini, "On the cooperative exploitation of antenna sensitivity and auto-tuning capability of UHF RFID chip. application to temperature sensing," in *2018 IEEE/MTT-S International Microwave Symposium - IMS*, Philadelphia, PA, Jun. 2018, pp. 374–377.

[7] K. Zannas, H. El Matbouly, Y. Duroc, and S. Tedjini, "Self-tuning RFID tag: A new approach for temperature sensing," *IEEE Transactions on Microwave Theory and Techniques*, vol. 66, no. 12, pp. 5885–5893, Nov. 2018.

[8] X. Zhang, H.-X. Li, and H. S.-H. Chung, "Setup-independent UHF RFID sensing technique using multidimensional differential measurement," *IEEE Internet of Things Journal*, vol. 8, no. 13, pp. 10 509–10 517, Jul. 2021.

[9] R. Bhattacharyya, F. Villa Gonzalez, and P. Nikitin, "Material sensing using RAIN RFID tags with auto-tuning capabilities," *IEEE Journal of Radio Frequency Identification*, vol. 9, pp. 340–349, May 2025.

[10] Remote Antenna Impedance Estimation. [Online]. Available: https://github.com/nicolas-barbot/Antenna_Impedance_Estimation

[11] J. Mayhan, A. Dion, and A. Simmons, "A technique for measuring antenna drive port impedance using backscatter data," *IEEE Transactions on Antennas and Propagation*, vol. 42, no. 4, pp. 526–533, Apr. 1994.

[12] P. Pursula, D. Sandstrom, and K. Jaakkola, "Backscattering-based measurement of reactive antenna input impedance," *IEEE Transactions on Antennas and Propagation*, vol. 56, no. 2, pp. 469–474, Feb. 2008.

[13] J. Romeu, S. Capdevila, J. Bolomey, and L. Jofre, "Antenna input impedance measurement using multi-load MST," in *2013 International Workshop on Antenna Technology (iWAT)*, Karlsruhe, Germany, Mar. 2013, pp. 353–356.

[14] S. Capdevila, L. Jofre, J. Romeu, and J. C. Bolomey, "Multi-loaded modulated scatterer technique for sensing applications," *IEEE Transactions on Instrumentation and Measurement*, vol. 62, no. 4, pp. 794–805, Apr. 2013.

[15] P. del Hougne, "Virtual VNA: Minimal-ambiguity scattering matrix estimation with a fixed set of "virtual" load-tunable ports," *IEEE Transactions on Instrumentation and Measurement*, vol. 74, pp. 1–19, Mar. 2025.

[16] ——, "Virtual VNA 2.0: Ambiguity-free scattering matrix estimation by terminating not-directly-accessible ports with tunable and coupled loads," *IEEE Transactions on Antennas and Propagation*, vol. 73, no. 7, pp. 4903–4908, Jul. 2025.

[17] ——, "Virtual VNA 3.0: Unambiguous scattering matrix estimation for nonreciprocal systems by leveraging tunable and coupled loads," *IEEE Transactions on Instrumentation and Measurement*, vol. 74, pp. 1–15, Aug. 2025.

[18] ——, "Wireless multi-port sensing: Virtual-VNA-enabled de-embedding of an over-the-air fixture," *IEEE Transactions on Antennas and Propagation*, pp. 1–1, Dec. 2025.

[19] R. B. Green, "The general theory of antenna scattering," Ph.D. dissertation, The Ohio State University, Electrical Engineering., OH, USA, 1963.

[20] N. Barbot and M. Reynolds, "A general receiver for backscatter signals: A step-by-step tutorial," *IEEE Microwave Magazine*, pp. 2–14, Aug. 2025.

[21] J. Grosinger, "What's your take on chips? Chip impedance measurement practice for RF energy harvesting," *IEEE Microwave Magazine*, vol. 26, no. 4, pp. 76–82, Apr. 2025.

[22] P. Nikitin, J. Kim, and K. Rao, "RFID tag analysis using an equivalent circuit," in *2021 IEEE International Symposium on Antennas and Propagation and USNC-URSI Radio Science Meeting (APS/URSI)*, Singapore, Singapore, Dec. 2021, pp. 167–168.

[23] N. Barbot and V. C. V, "Open testing and measurement bench for UHF RFID," in *2023 IEEE 13th International Conference on RFID Technology and Applications (RFID-TA)*, Aviero, Portugal, Sep. 2023, pp. 158–161.

[24] P. Nikitin, J. Kim, and K. V. S. Rao, "Analysis of UHF RFID tag antennas using an equivalent circuit approach," *IEEE Journal of Radio Frequency Identification*, vol. 10, pp. 136–149, Feb. 2026.

[25] L. J. Görtschacher and J. Grosinger, "UHF RFID sensor system using tag signal patterns: Prototype system," *IEEE Antennas and Wireless Propagation Letters*, vol. 18, no. 10, pp. 2209–2213, Oct. 2019.

[26] E. A. Keehr and G. Lasser, "Making a low-cost software-defined UHF RFID reader," *IEEE Microwave Magazine*, vol. 22, no. 3, pp. 25–45, 2021.